Article

Rab27A and its effector MyRIP link secretory granules to F-actin and control their motion towards release sites

Claire Desnos,[1] Jean-Sébastien Schonn,[1] Sébastien Huet,[1] Viet Samuel Tran,[1] Aziz El-Amraoui,[2] Graça Raposo,[3] Isabelle Fanget,[1] Catherine Chapuis,[1] Gaël Ménasché,[4] Geneviève de Saint Basile,[4] Christine Petit,[2] Sophie Cribier,[5] Jean-Pierre Henry,[1] and François Darchen[1]

[1]Centre National de la Recherche Scientifique (CNRS) UPR 1929, Institut de Biologie Physico-Chimique, 75005 Paris, France
[2]CNRS URA 1968, Institut Pasteur, 75724 Paris cedex 15, France
[3]UMR 144 Curie/CNRS, Institut Curie, 75248 Paris cedex 05, France
[4]Institut National de la Santé et de la Recherche Médicale U429, Hôpital Necker, 75743 Paris cedex 15, France
[5]CNRS UMR 7099, Institut de Biologie Physico-Chimique, 75005 Paris, France

The GTPase Rab27A interacts with myosin-VIIa and myosin-Va via MyRIP or melanophilin and mediates melanosome binding to actin. Here we show that Rab27A and MyRIP are associated with secretory granules (SGs) in adrenal chromaffin cells and PC12 cells. Overexpression of Rab27A, GTPase-deficient Rab27A-Q78L, or MyRIP reduced secretory responses of PC12 cells. Amperometric recordings of single adrenal chromaffin cells revealed that Rab27A-Q78L and MyRIP reduced the sustained component of release. Moreover, these effects on secretion were partly suppressed by the actin-depolymerizing drug latrunculin but strengthened by jasplakinolide, which stabilizes the actin cortex. Finally, MyRIP and Rab27A-Q78L restricted the motion of SGs in the subplasmalemmal region of PC12 cells, as measured by evanescent-wave fluorescence microscopy. In contrast, the Rab27A-binding domain of MyRIP and a MyRIP construct that interacts with myosin-Va but not with actin increased the mobility of SGs. We propose that Rab27A and MyRIP link SGs to F-actin and control their motion toward release sites through the actin cortex.

Introduction

Hormones and neuropeptides are stored in secretory granules (SGs) and released by exocytosis in response to cytosolic calcium elevation. SGs are formed at the TGN as short-lived vesicular intermediates, termed immature SGs, and transported along microtubules to the cell periphery. Immature SGs are then restricted to the cell periphery within the actin cortex, a dense network of actin filaments, where they mature completely (Rudolf et al., 2001). Thus, outward microtubule-dependent transport and F-actin–dependent capture mediate the cortical localization of SGs. However, if the actin cortex may favor peripheral localization of SGs, it may also hinder the access of vesicles to the plasma membrane. Indeed, the actin network has a mesh smaller than a granule diameter (Nakata and Hirokawa, 1992), and it would completely prevent exocytosis to occur if it were not dynamically remodeled or severed, in particular upon calcium influx. In adrenal chromaffin cells, exocytosis occurs preferentially at sites where the actin cortex has gaps, suggesting that cortical F-actin acts as a barrier that hampers fusion (Trifaro et al., 2000). Finally, actin filaments or actin bundles can also provide tracks on which SGs move in an energy-dependent manner (Lang et al., 2000; Oheim and Stuhmer, 2000). Whether F-actin promotes or restricts the mobility of SGs and their access to the plasma membrane will finally depend on the dynamics of microfilaments and on the physical interaction of SGs with F-actin.

A similar actin-dependent capture of the pigment-producing organelles, termed melanosomes, has been described in skin melanocytes (Wu et al., 1998), and a detailed molecular mechanism has been recently provided. The GTP-binding protein Rab27A, which is associated with the membrane of melanosomes, recruits melanophilin, the product of *MLPH*, which in turn recruits myosin-VA (Fukuda et al., 2002b;

Abbreviations used in this paper: 5-HT, 5-hydroxytryptamine; CTL, cytotoxic T lymphocyte; EW-FM, evanescent wave fluorescence microscopy; hGH, human growth hormone; MSD, mean square displacement; NPY, neuropeptide Y; SERT, serotonin transporter; SG, secretory granule.

Figure 1. **Localization of Rab27A on SGs by confocal immunofluorescence.** Chromaffin cells (A–C) were double imaged for endogenous Rab27A (A) and chromogranin A/B (B). Discrete punctate structures were observed in A and B; most of them precisely coincided. See the overlaid image (C) and the detail shown at higher magnification (inset). Anti-Rab27A (D) and anti–chromogranin A/B (E) also stained discrete structures that coincided (F, overlay) in PC12 cells. GFP–Rab27A (G) transiently expressed in NGF-treated PC12 cells also colocalized with chromogranin B–positive structures (H) (I, overlaid image). Note the enrichment of Rab27A and chromogranin B at the tip of neurites. In contrast, Rab27A (J) did not colocalize with LYAAT, a lysosomal marker (K and L). Bars, 5 μm.
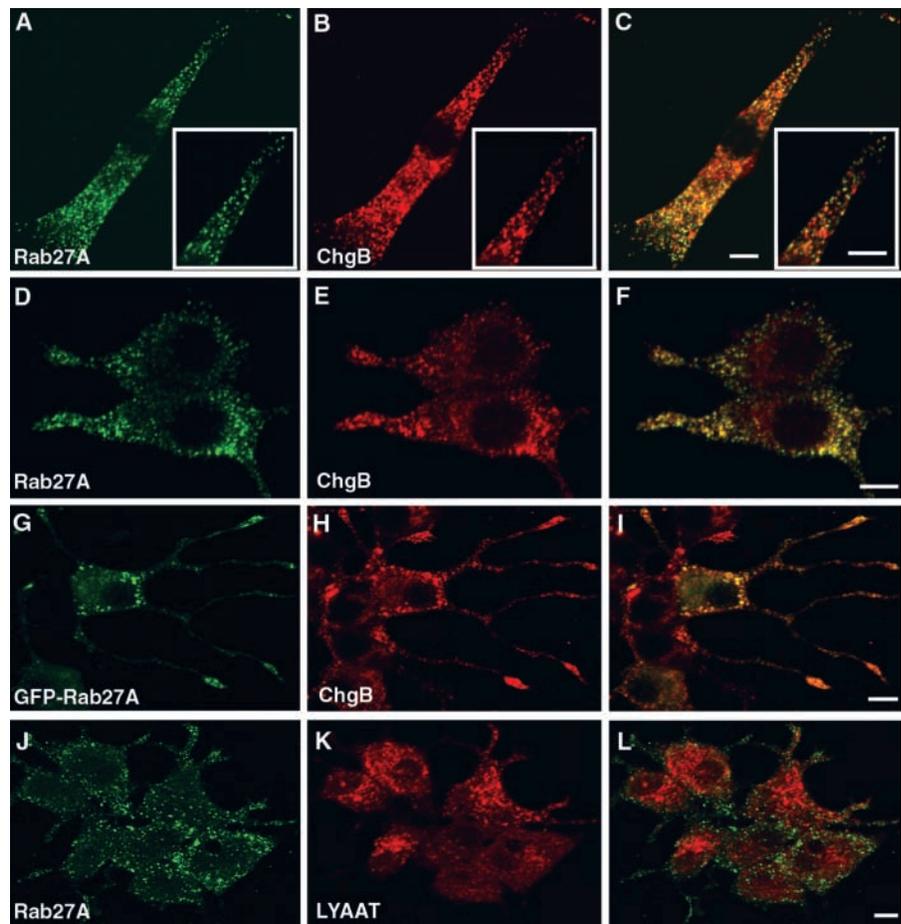
Hume et al., 2002; Strom et al., 2002; Wu et al., 2002). In humans, mutations in *RAB27A* cause Griscelli syndrome, an autosomal recessive disorder characterized by partial albinism and uncontrolled T lymphocyte and macrophage activation (hemophagocytic syndrome) (Ménasché et al., 2000). In melanocytes isolated from these patients or from *ashen* mice bearing loss-of-function mutations in Rab27A, melanosomes are concentrated in the perinuclear region and cannot accumulate at the distal ends of the dendritic extensions (Wilson et al., 2000; Bahadoran et al., 2001; Hume et al., 2001; Wu et al., 2001). Consequently, melanin cannot be transferred to keratinocytes. Similar impairment of melanosome transport is observed in *leaden* and *dilute* mice bearing mutations in *MLPH* (Matesic et al., 2001) and in *MYO5a* (Strobel et al., 1990; Provance et al., 1996), respectively. These observations indicate that Rab27A, melanophilin, and myosin-VA mediate the physical link between melanosomes and F-actin.

In retinal pigment epithelial cells, another melanosome-associated complex made of Rab27A, MyRIP, and myosin-VIIA was described recently (El-Amraoui et al., 2002). MyRIP was found to have a broad tissular distribution (Fukuda and Kuroda, 2002), suggesting that its function may not be restricted to melanosome trafficking. In particular, MyRIP is expressed in the retinal synaptic region and, upon expression in pheochromocytoma PC12 cells, was targeted to the tip of neurites that were enriched in SGs. These observations suggested that Rab27A and MyRIP could have a role in secretory vesicle trafficking. Consistently, the activity of Griscelli and *ashen* cy-

totoxic T lymphocytes (CTLs) is reduced due to a defect in lytic granule secretion (Ménasché et al., 2000; Haddad et al., 2001; Stinchcombe et al., 2001). Moreover, Rab27A is associated with insulin-containing granules (Yi et al., 2002).

Here we report that Rab27A and MyRIP are associated with large dense core granules in adrenal chromaffin cells and pheochromocytoma PC12 cells and control the secretory activity in a manner that depends on the state of the actin cortex. Moreover, they reduce the mobility of SGs beneath the plasma membrane. The results are consistent with Rab27A and MyRIP bridging vesicles to F-actin and regulating the movement of vesicles within the actin cortex.

Results

Association of Rab27A and MyRIP with SGs

Upon overexpression in PC12 cells, MyRIP was previously found to be targeted to the tip of neurites where SGs accumulate (El Amraoui et al., 2002). These observations suggested that Rab27A might be responsible for the recruitment of MyRIP not only on melanosomes but also on SGs. Therefore, the expression and subcellular localization of Rab27A and MyRIP were investigated. The monoclonal anti-Rab27A antibody used in this study did not react with purified recombinant Rab3A, B, C, and D, or with Rab4, Rab11, or GFP–Rab27B transiently expressed in COS-7 cells (unpublished data). Using this antibody, we detected Rab27A in bovine adrenal chromaffin cells and in PC12 cells.
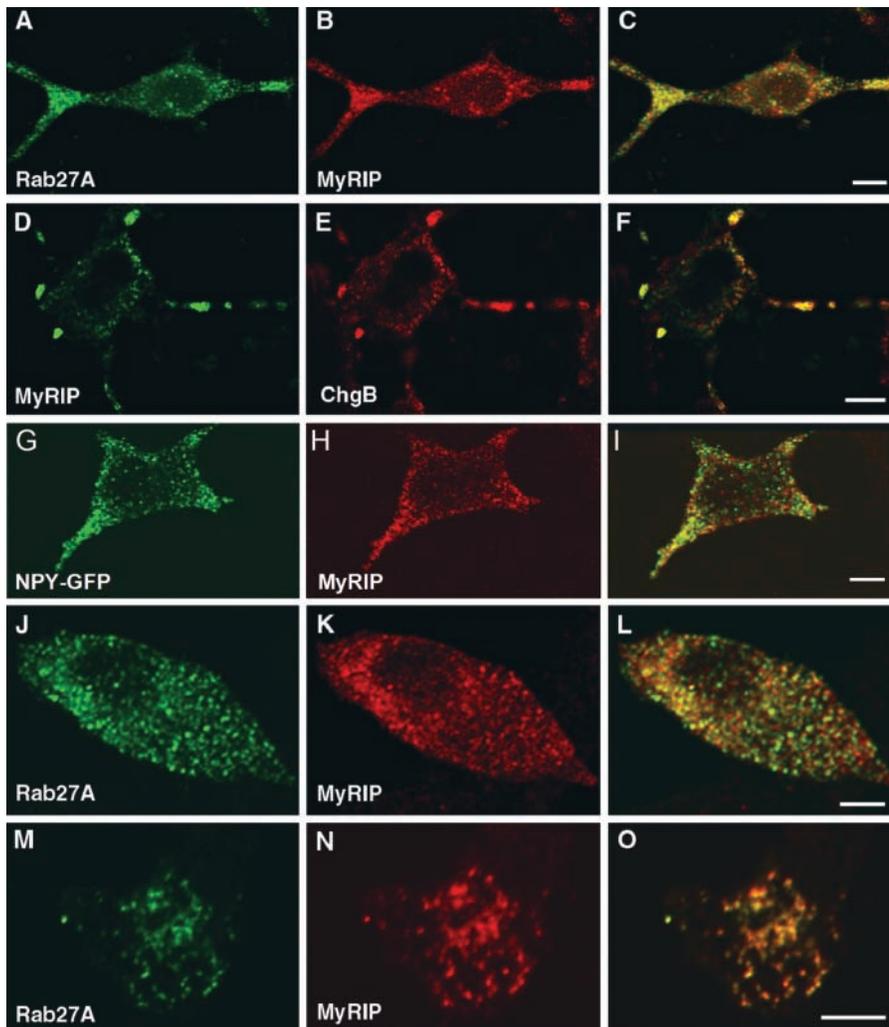
Figure 2. **Confocal immunofluorescence localization of MyRIP on SGs.** PC12 cells (A–I) were double imaged for endogenous Rab27A (A) and MyRIP (B) showing discrete punctate structures; most of these structures coincided (C, overlaid image), especially in the neurites. PC12 cells were transfected with pCMV-MyRIP and double imaged for MyRIP (D and H) and chromogranin B (E) or NPY–GFP (G); overlaid images indicate that MyRIP colocalized partly with chromogranin B (F) and NPY–GFP (I). Chromaffin cells (J–O) were imaged for endogenous Rab27A (J and M) and MyRIP (K and N). Many structures were double labeled, as indicated by the overlaid image of a cell sectioned close to the apex (O). Bars, 5 μm.

The subcellular localization of Rab27A was investigated by cell fractionation of chromaffin cells. The protein was hardly detectable in the cytosol. A crude membrane fraction was separated on a sucrose gradient. Rab27A, the vesicular monoamine transporter VMAT2 and the v-SNARE protein VAMP2 were enriched in the same dense fractions of the gradient, consistent with an association of Rab27A with SGs (Fig. S1, available at http://www.jcb.org/cgi/content/full/jcb.200302157/DC1). In contrast, the distribution of Rab27A was not similar to that of lysosomal β-glucuronidase. MyRIP was detected in chromaffin and PC12 cell extracts as a single band (∼96 kD) but was not detected in gradient fractions, presumably because its membrane association is rather labile. Next, the localization of Rab27A and MyRIP was studied by confocal fluorescence microscopy. Chromaffin cells labeled with anti-Rab27A antibodies displayed a punctated labeling distributed throughout the cytoplasm. Moreover, most of the Rab27A-positive structures were also decorated by an antiserum raised against chromogranin A/B, a component of SG matrix (Fig. 1, A–C), and by an anti–dopamine β-hydroxylase, a marker of SG membrane (not depicted). The distribution of Rab27A was also analyzed in NGF-differentiated PC12 cells. As illustrated in Fig. 1 (D–F), the overall distribution of Rab27A was very similar to that of SGs (stained by an anti–chromogranin A/B antiserum), with a marked enrichment at the tip of neurites. Also,

GFP-tagged Rab27A was expressed in PC12 cells, and its localization was very similar to that of chromogranin B, stained with a monoclonal antibody (Fig. 1, G–I). In contrast, LYAAT, an amino acid lysosomal transporter (Sagné et al., 2001), displayed a very different intracellular distribution (Fig. 1, J–L). Together these results indicate that Rab27A is associated with SGs.

Next, we investigated the localization of the Rab27A effector MyRIP by confocal fluorescence microscopy. In NGF-differentiated PC12 cells, endogenous MyRIP displayed a punctate distribution very similar to that of Rab27A (Fig. 2, A–C). In addition, overexpressed MyRIP was targeted to SGs, as indicated by colocalization of MyRIP with chromogranin B (Fig. 2, D–F) and neuropeptide Y (NPY)–GFP (Fig. 2, G–I). In contrast, no significant overlap was observed between MyRIP and synaptophysin, a marker of early endosomes and synaptic-like microvesicles (not depicted). In chromaffin cells, endogenous MyRIP also displayed a punctated distribution evenly distributed throughout the cytoplasm. When the cells were double imaged for MyRIP and Rab27A, many structures contained both markers (Fig. 2, J–L). This is even more evident in Fig. 2 (M–O), which shows an apical section of a chromaffin cell. Fewer structures could be seen, and almost all of them contain both MyRIP and Rab27A. The complete overlap of the two markers in this
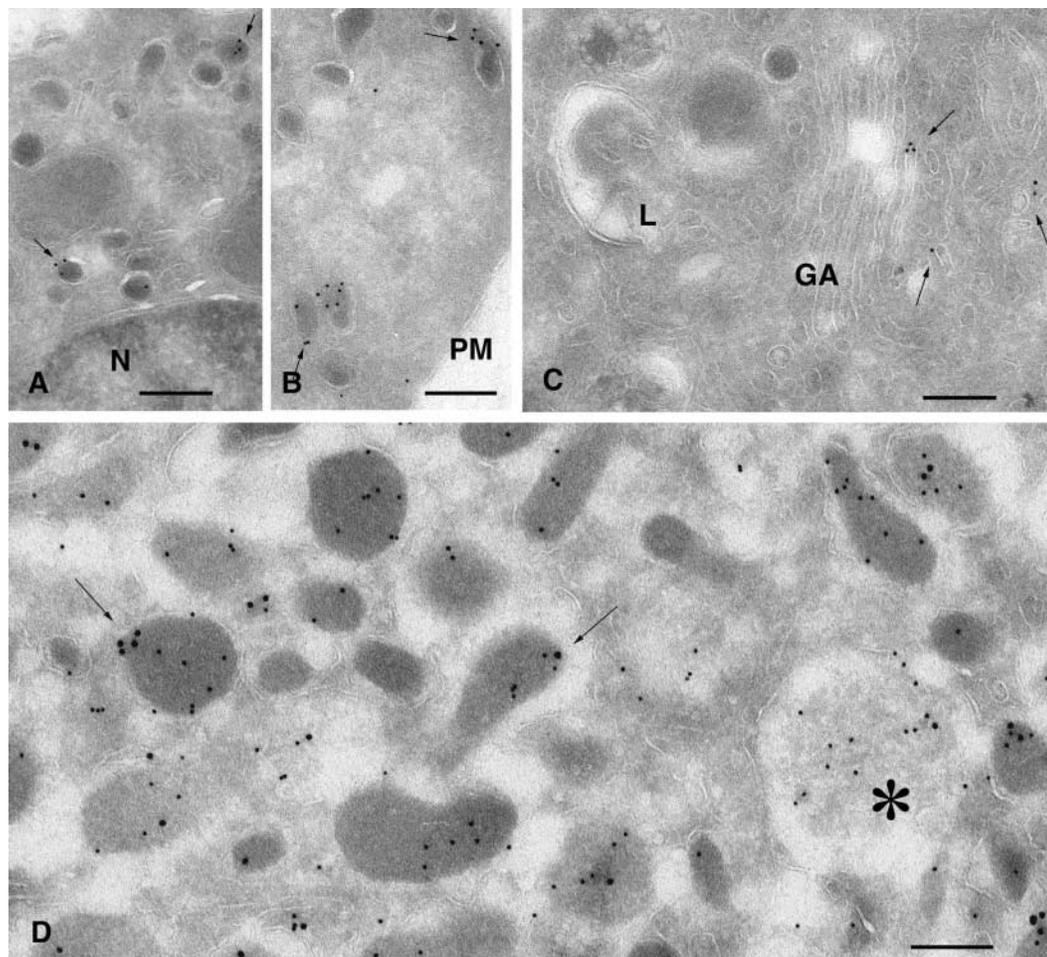
Figure 3.   **Ultrastructural localization of Rab27A in PC12 and chromaffin cells.** Ultrathin cryosections of PC12 (A–C) and chromaffin cells (D) were single or double immunogold labeled for Rab27A (10-nm gold particles, A–C) or Rab27A (15-nm gold particles, D) and chromogranin A/B (10-nm gold particles, D). (A and B) Specific labeling of dense core granules of PC12 cells with anti-Rab27A antibodies. A restricted number of dense granules show high density of labeling for Rab27A (arrows), whereas others are negative. (C) Rab27A-positive tubulo-vesicular structures (arrows) are often observed in the Golgi region. (D) In chromaffin cells, Rab27A localizes to chromogranin-positive SGs (arrows) and to immature granules (star). N, nucleus; PM, plasma membrane; GA, Golgi apparatus. Bars, 200 nm.

section might suggest that the colocalization of MyRIP and Rab27A is better at the cell periphery. This is consistent with results obtained in PC12 cells, where MyRIP was also found on somatic structures that were not stained with anti-chromogranin or anti-Rab27A antibodies.

Finally, the localization of Rab27A was analyzed at the ultrastructural level on ultrathin cryosections of PC12 and chromaffin cells. Endogenous MyRIP could not be detected by immunoelectron microscopy with our antibodies. In PC12 cells, the majority of Rab27A-bound gold particles was associated with SGs, identified according to their electron-dense matrix and their size (Fig. 3, A and B). Rab27A labeling was also found in tubulo-vesicular structures close to the Golgi apparatus, as illustrated in Fig. 3 C. These observations suggest that Rab27A may have a role at different sites in the secretory pathway. Quantitative analysis of several sections of PC12 cells revealed that ∼92% of Rab27A-associated gold particles were found on SGs and 8% on vesicles or tubulo-vesicular profiles located in the vicinity of the Golgi apparatus; 15% of SGs were depicted with greater than four gold particles. Double labeling of sections of chromaffin cells with anti-Rab27A

(15-nm gold particles) and anti-chromogranin (10-nm gold particles) antibodies revealed a specific association of Rab27A with SGs (Fig. 3 D). In addition, some immature granules were labeled (Fig. 3 D, asterisk). Some Rab27A-associated gold particles seemed to be located within SGs. This was observed also with another anti-Rab27A monoclonal antibody and in melanosomes (not depicted), suggesting that this observation is physiologically relevant. Previous reports showed within SGs the presence of vesicles, reminiscent of exosomes (Denzer et al., 2000), that are released in the external milieu during exocytosis (Ornberg et al., 1986).

Interaction of MyRIP with myosin-Va and actin

MyRIP was initially identified as a ligand of myosin-VIIa. However, myosin-VIIa was not detected in chromaffin and PC12 cells (unpublished data). In contrast, myosin-Va is expressed in chromaffin and PC12 cells, and its association with SGs was recently demonstrated (Rosé et al., 2003; Rudolf et al., 2003). Moreover, Fukuda and Kuroda (2002) found an interaction between full-length MyRIP and myosin-Va. We confirmed this observation using purified GST-tagged
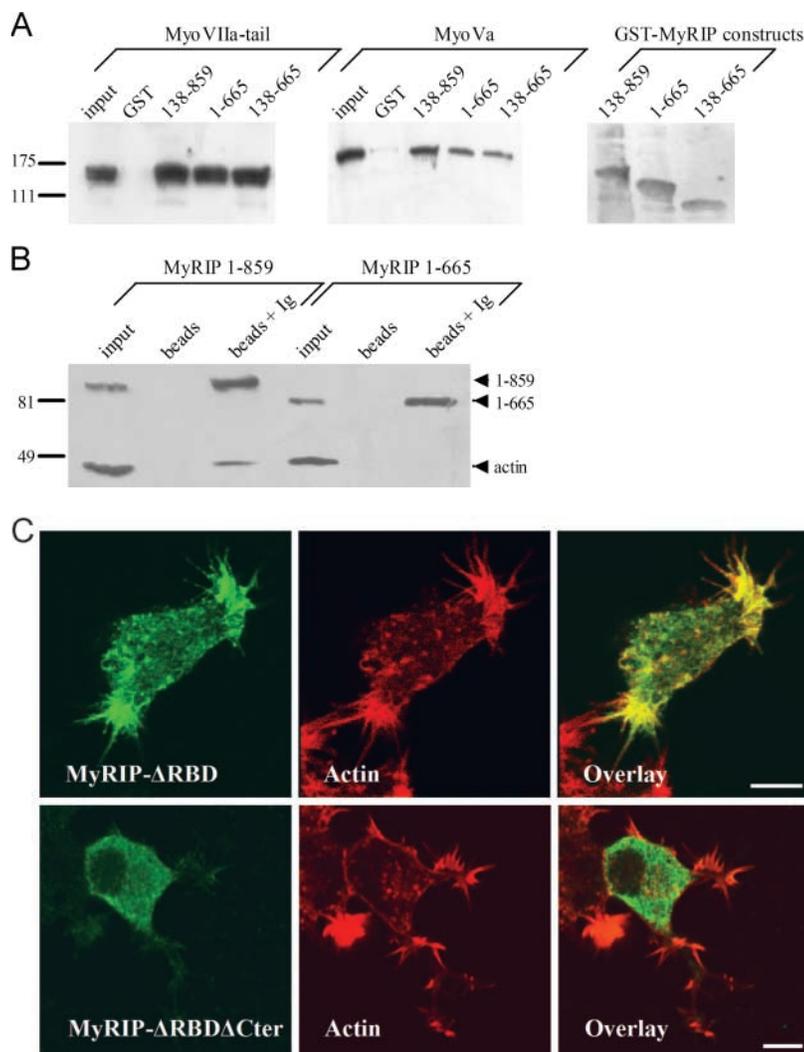
Figure 4. **Interaction of MyRIP with myosin-Va and actin.** (A) Binding of myosin-VIIa tail (left) or myosin-Va (middle) to purified GST or GST–MyRIP constructs immobilized on glutathione–Sepharose beads. Transfected COS-7 cells and nontransfected PC12 cells were used as a source of myosin-VIIa and myosin-Va, respectively. Cellular levels of myosin-VIIa and myosin-Va are shown in the first lane of each panel (input, 10% of the volume used in the experiment). The position of molecular weight markers is shown on the left side ($\times 10^{-3}$). The same blots were stripped and reprobed with an anti-GST monoclonal antibody to reveal the MyRIP constructs bound to the beads (right). Note that deletion of the COOH-terminal region of MyRIP had little effect on the interaction with myosins. Similar results were obtained in another experiment. (B) The COOH-terminal region of MyRIP is required for actin binding. COS-7 cells were transfected with vectors encoding full-length MyRIP (1–859) or a deletion mutant (1–665). The proteins expressed were immunoprecipitated with anti-MyRIP antibody–conjugated protein A–Sepharose (beads + Ig). Coimmunoprecipitated actin was revealed with a monoclonal antibody. Beads without antibody were used as control (beads). The amount of expressed MyRIP proteins used in the immunoprecipitation is shown on the left (input, 1/8 of the volume used). Similar results were obtained in another experiment. (C) Importance of the COOH-terminal region of MyRIP for its colocalization with F-actin. PC12 cells were transfected with MyRIP-ΔRBD (138–859) (top) or MyRIP-ΔRBD-ΔCter (138–665) (bottom). 3 d later, cells were stained with anti–myc tag antibodies (left) or rhodamine-phalloidin (middle) and imaged by confocal immunofluorescence. The overlaid images (right) show that MyRIP-ΔRBD, but not MyRIP-ΔRBD-ΔCter, colocalizes with F-actin.

MyRIP constructs. GST–MyRIP-ΔCter (1–665) and ΔRBD-ΔCter (138–665) interacted with the tail of myosin-VIIa and with myosin-Va (Fig. 4 A). However, the myosin-VIIa– and myosin-Va–binding domains of MyRIP do not overlap completely, as MyRIP (1–577) bound to myosin-VIIa (El Amraoui et al., 2002) but poorly to myosin-Va (not depicted). Fukuda and Kuroda (2002) also found an interaction between MyRIP and actin by coimmunoprecipitation. Deletion of residues 666–859 had little effect on myosin-Va binding (Fig. 4 A) but completely abolished the interaction with actin (Fig. 4 B). The importance of this COOH-terminal region for actin binding was also demonstrated by immunocytochemistry (Fig. 4 C). A deletion mutant of MyRIP lacking the Rab27a-binding domain (MyRIP-ΔRBD) colocalized with actin, whereas MyRIP-ΔRBD-ΔCter (138–665), lacking also the COOH-terminal region required for in vitro actin binding, gave a diffuse cytosolic staining. This region has significant sequence similarity with melanophilin, which was shown to bind actin directly (Fukuda and Kuroda, 2002).

A role for Rab27A and MyRIP in SG exocytosis
Overexpressed Rab27A and MyRIP inhibited secretory responses of PC12 cells. Then, we investigated whether Rab27a and MyRIP may control the secretory activity of

PC12 cells. The effect of various constructs was analyzed at the cell population level by means of two secretion assays based on cotransfection of vectors encoding either a serotonin transporter (SERT) or human growth hormone (hGH). Due to the very high increase in tritiated 5-hydroxytryptamine ([^{3}H]5-HT) uptake induced by SERT, the subpopulation of transfected cells can be specifically labeled and its secretory activity determined by measuring release of [^{3}H]5-HT (Schonn et al., 2003). hGH is properly targeted to SGs and released in response to Ca^{2+} elevation (Wick et al., 1993).

Rab GTPases switch between active GTP-bound and inactive GDP-bound conformations. To investigate the function of Rab27A in regulated secretion, wild-type Rab27A or mutants defective in GTP binding (T23N) or in GTPase activity (Q78L) were transiently expressed in PC12 cells. Rab27A-T23N was supposed to interfere with the function of endogenous protein by competing for a guanine nucleotide exchange factor that catalyzes the exchange of GTP for GDP. Rab27A-Q78L was used to increase levels of active GTP-bound Rab27A. Overexpressed Rab27A and Rab27A-Q78L displayed a punctated distribution very similar to that of endogenous Rab27A (Fig. 1, G–I; Fig. S2, available at http://www.jcb.org/cgi/content/full/jcb.200302157/DC1). In contrast, Rab27A-T23N gave a diffuse staining of the cytosol (Fig.

Figure 6. **MyRIP controls the magnitude of secretory responses.** SERT-transfected (black bars) or hGH-transfected PC12 cells (gray bars) were cotransfected with vectors encoding wild-type MyRIP (MyRIP 1–859), the Rab27A binding domain of MyRIP (MyRIP 1–134), a construct lacking the RBD (138–859), or MyRIP-ΔCter (1–665). Cells were incubated for 10 min in normal or high K+ saline. Release in normal saline medium was subtracted. Results are shown as percentage of the response of mock-transfected cells (mean ± SEM). The number of experiments performed is shown above the bars.
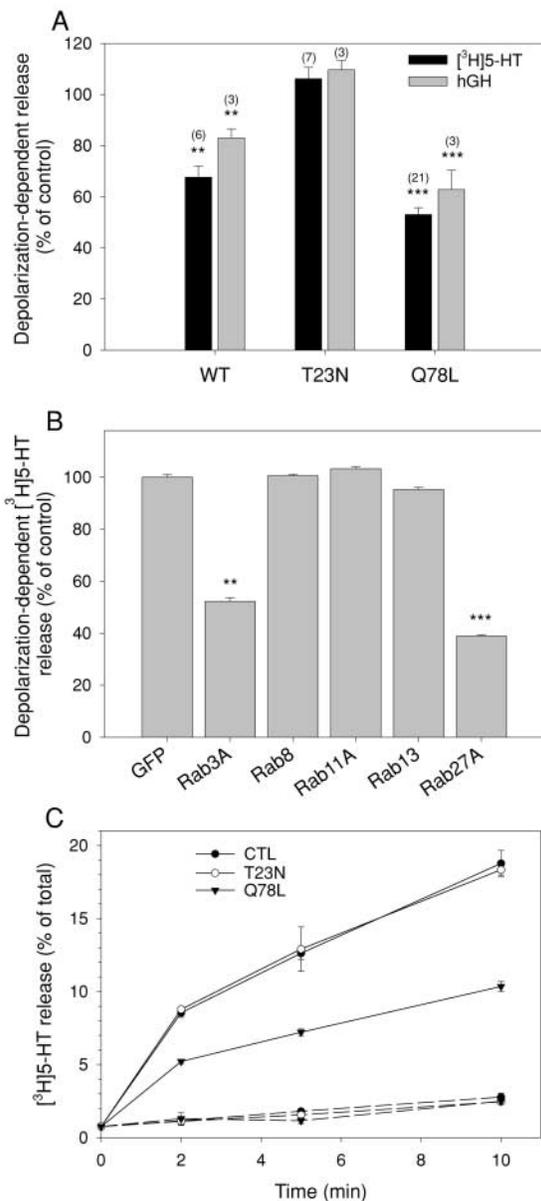
Figure 5. **Rab27A controls the magnitude of secretory responses.** (A) SERT-transfected (black bars) or hGH-transfected PC12 cells (gray bars) were cotransfected with vectors encoding untagged Rab27A wild type, Rab27A-T23N, or Rab27A-Q78L, as indicated. Cells were incubated for 10 min in normal or high K+ saline. Release in normal saline medium (2–5% of cellular [3H]5-HT) was subtracted. Results are shown as percentage of the responses of mock-transfected cells. Numbers in brackets refer to the number of independent experiments. The stimulus-dependent release of control cells ranged from 15 to 30% of cellular [3H]5-HT (mean ≈ 20%). (B) Effect of GTPase-deficient Rab3A, Rab8, Rab11, and Rab13 on secretory responses measured as in A. Rab8, Rab11, Rab13, and Rab27A were fused to GFP. Transfection of GFP was used as a control. Results are shown as percentage of the depolarization-dependent [3H]5-HT release from control cells (mean ± SEM, $n = 3$ independent experiments). Whereas Rab3A-Q81L and GFP–Rab27A-Q78L inhibit PC12 cell stimulated exocytosis, no effect was observed upon overexpression of GFP-tagged GTPase-deficient Rab8, Rab11, or Rab13. (C) [3H]5-HT release as a function of time from control cells (●) or from cells expressing Rab27A-T23N (○) or Rab27A-Q78L (▼). Cells were incubated in normal (dotted line) or high K+ saline (plain line). Results are expressed in percentage (mean ± SEM, $n = 3$) of total [3H]5-HT present in the cells before stimulation. Similar results were obtained in two other independent experiments.
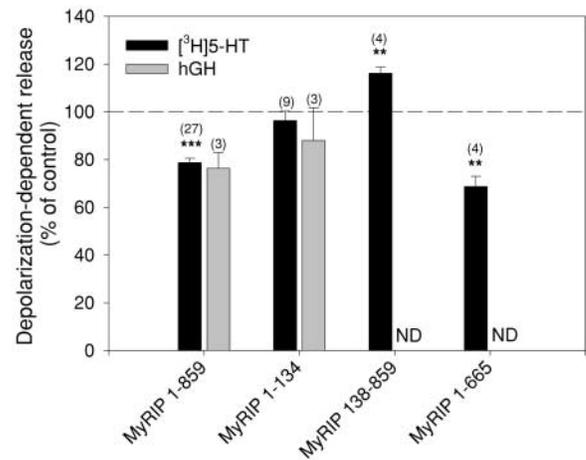
S2). Rab27A-T23N did not induce any significant change of secretory activity. In contrast, GTPase-deficient Rab27A-Q78L and, to a less extent, wild-type Rab27A have a pronounced inhibitory effect on secretion (Fig. 5 A). Similar effects of Rab27A proteins were observed in cells permeabilized with α-toxin or streptolysin-O (Rab27A WT: −24 ± 6.5%, mean ± SEM, $n = 5$ experiments; Rab27A-Q78L: −57 ± 4.6%, mean ± SEM, $n = 3$ experiments). As these pore-forming toxins bypass voltage-dependent calcium channels, the inhibitory effect of Rab27A was not due to reduced Ca^{2+} influx. Rab27A-Q78L inhibited secretory responses over a wide range of free calcium concentrations without apparent shift in the calcium sensitivity of the secretory apparatus (unpublished data). The effect of Rab27A-Q78L was compared with that of other GTPase-deficient Rab proteins. Rab3A-Q81L inhibited secretion as previously reported (Johannes et al., 1994; Schonn et al., 2003), but GFP-tagged Rab8, Rab11, and Rab13 did not interfere with the secretory activity of PC12 cells (Fig. 5 B), although they were properly expressed (Fig. S3, available at http://www.jcb.org/cgi/content/full/jcb.200302157/DC1). Thus, the effect of Rab27A on exocytosis is specific.

Next, we investigated the effect of MyRIP on secretory responses. Overexpression of full-length MyRIP or of MyRIP-ΔCter (1–665) induced moderate but reproducible reduction of the secretory activity of PC12 cells (Fig. 6). In contrast, overexpression of MyRIP-ΔRBD (138–859) slightly increased secretory responses, while MyRIP-RBD (1–134) had no significant effect (Fig. 6).

Kinetics of secretory responses. To investigate the site of action of Rab27A-Q78L, the time course of its effect was investigated. As illustrated in Fig. 5 C, Rab27A-Q78L had similar inhibitory effects at various time points (2, 5, and 10 min of stimulation). Similar results were obtained for MyRIP (not depicted). The kinetics of secretory responses was determined
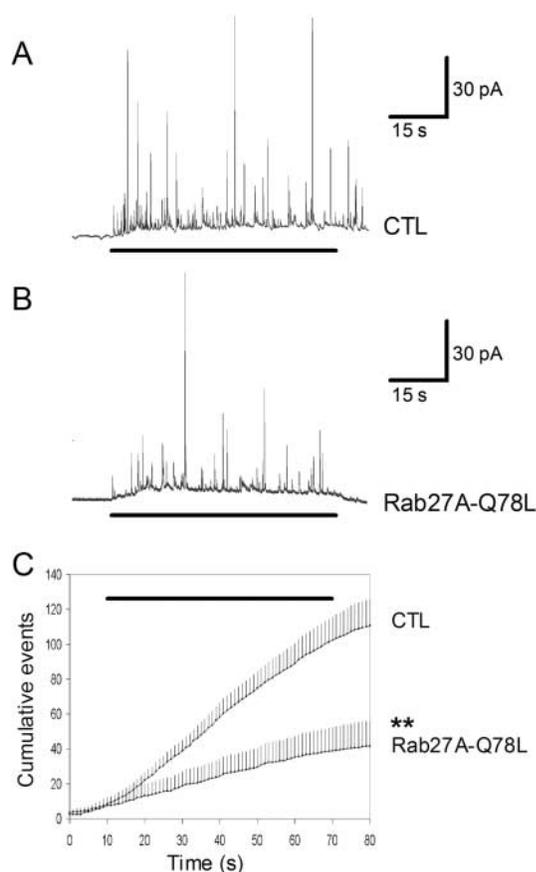
Figure 7. **Rab27A-Q78L reduces the frequency of amperometric spikes in chromaffin cells.** Secretory responses of single adrenal chromaffin cells were monitored by carbon fiber amperometry. (A) Amperometric trace recorded from a GFP-transfected (CTL) chromaffin cell stimulated by local application of 10 μM nicotine (indicated by the bar below the trace). (B) Secretory response of a Rab27A-Q78L–expressing cell. (C) The cumulative number of spikes is plotted against time. Shown are the mean values (+SEM) from 17 cells (CTL) and 6 cells (Rab27A-Q78L). The bar above the traces indicates the presence of nicotine. The significance of difference was calculated with Mann-Whitney test.

Figure 8. **Overexpression of MyRIP reduces the frequency of amperometric spikes in chromaffin cells.** Secretory responses of single adrenal chromaffin cells were monitored by carbon fiber amperometry. (A) Amperometric trace recorded from a GFP-transfected (CTL) chromaffin cell stimulated by local application of high K$^+$ (55 mM) saline (indicated by bars below the trace). (B) Secretory responses of a wild-type MyRIP (MyRIP-FL)–transfected cell. (C) The cumulative number of spikes is plotted against time. Shown are the mean values (+SEM) from 18 cells (CTL) and 16 cells (MyRIP-FL). The bars indicate the application of high K$^+$. The significance of difference was calculated with Mann-Whitney test.

more accurately by means of carbon fiber amperometry on single chromaffin cells. Exocytosis is resolved by this technique as a series of current spikes, each spike being produced by the oxidation of the content of a single vesicle (Wightman et al., 1991). Chromaffin cells were cotransfected with Rab27A-Q78L or MyRIP and GFP (the latter being used to identify transfected cells). Cells expressing GFP only were used as controls. Overexpression of Rab27A-Q78L (Fig. 7) or MyRIP (Fig. 8) induced a significant reduction in spike frequency consistent with a reduction of the sustained phase of the release process. Rab27A and MyRIP might be implicated in the motion of vesicles toward the plasma membrane, the docking step, or the priming reaction, which makes vesicles ready to fuse.

Rab27A and MyRIP did not affect spontaneous release. We did not detect any increase in the spontaneous release of [³H]5-HT in Rab27A- or MyRIP-transfected cells compared with control cells during 10-min (Fig. 5 C) or 1-h (not depicted) incubations. However, as serotonin is not stably entrapped within SGs (Schonn et al., 2003), spontaneous release of [³H]5-HT during long periods of time
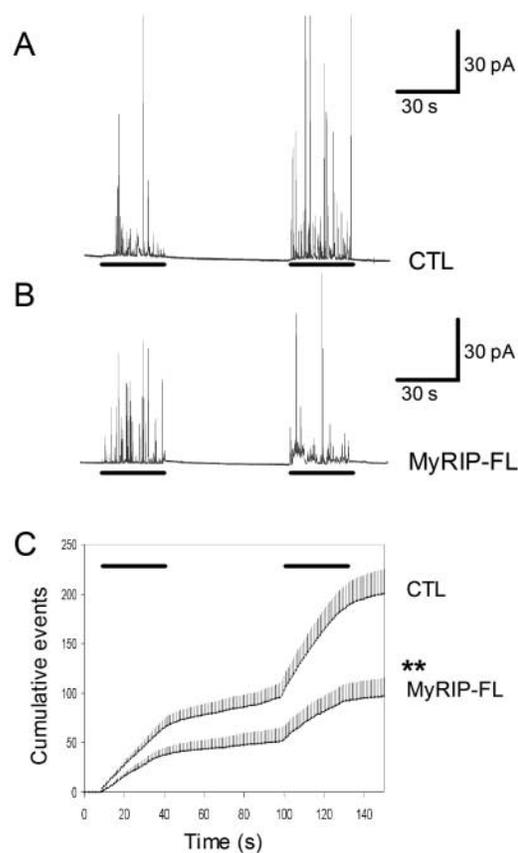
could not be used as a nonambiguous index of constitutive exocytosis. Released hGH was thus measured in the cell culture media 3 d after transfection. Compared with control cells, levels of hGH released from Rab27A WT– or Q78L-expressing cells were not significantly modified (not depicted). Furthermore, amperometric recordings did not detect any increase in spike frequency in the absence of stimulus (Figs. 7 and 8). These results suggest that the inhibitory effect of Rab27A and Rab27A-Q78L on secretory responses did not result from an increased release activity in resting conditions.

Secretory effects of Rab27A and MyRIP depend on the state of actin cortex

Biochemical data are consistent with a role for Rab27A and MyRIP in linking vesicles to F-actin. Entrapment of SGs within the actin cortex might thus be responsible for their inhibitory effect on secretory responses. To test this hypothesis, the effect of Rab27A and MyRIP on secretory responses was measured in cells treated with drugs that interfere with
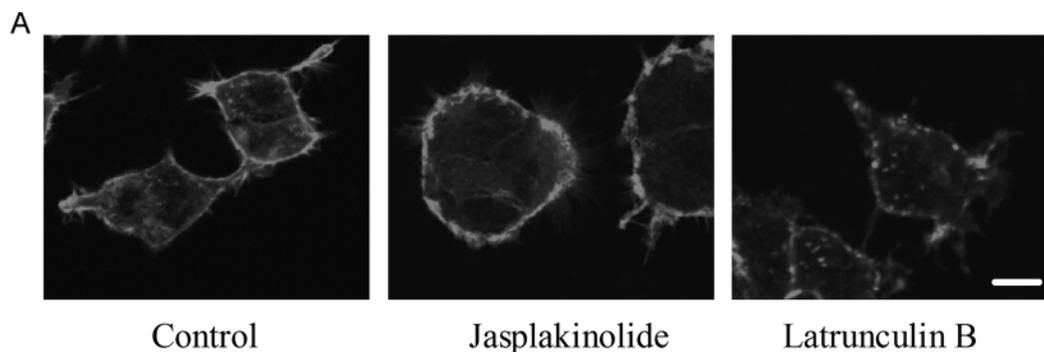
A

Control   Jasplakinolide   Latrunculin B

Figure 9. The effects of Rab27A-Q78L and MyRIP on secretion depend on the state of the actin cortex. (A) Rhodamine-phalloidin staining of the actin cortex of PC12 cells. Compared with control conditions (left), the thickness of actin is reduced upon latrunculin B treatment (middle) and increased by jasplakinolide (right). (B) The secretory activity of PC12 cells transfected with vectors encoding GFP (as control), Rab27A-Q78L, wild-type MyRIP (MyRIP 1–859), MyRIP-ΔCter (1–665), or granuphilin was measured as in Fig. 5 by means of the [³H]5-HT release assay. Cells were incubated without addition of drug (Std, black bars) or in the presence of 1 μM jasplakinolide (Jasp, open bars) or 5 μM latrunculin B (Lat B, gray bars) for 20 min before and during stimulation of secretion. The effect of the different proteins on secretion was expressed, after subtracting the basal release of [³H]5-HT in normal saline, as percentage of the stimulus-dependent secretory response of GFP-transfected cells measured under the same conditions (i.e., in the absence of drug, in the presence of jasp, or in the presence of lat B). Shown are the results (mean ± SEM) of several independent experiments (the number of experiments is shown above the bars). Latrunculin B significantly reduced (P < 0.001) the inhibitory effects of Rab27A-Q78L and MyRIP on secretion, whereas jasplakinolide increased that of MyRIP (P < 0.001). The net release of GFP-transfected cells was 19 ± 2% of cellular [³H]5-HT in the absence of drug, 20 ± 2.2% in the presence of jasplakinolide, and 31 ± 3% in the presence of latrunculin B.
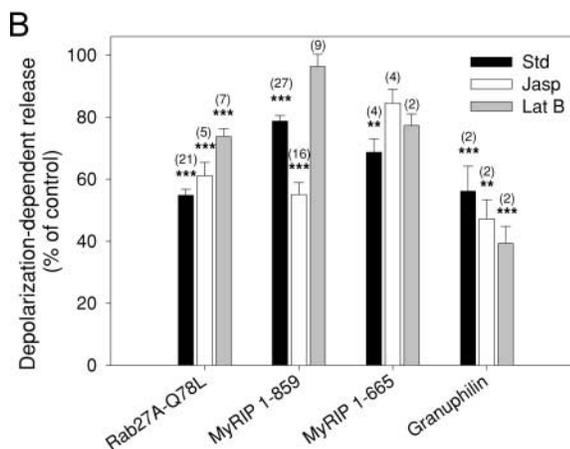
actin polymerization. Latrunculins favor actin depolymerization (Spector et al., 1983; Lang et al., 2000), whereas jasplakinolide promotes actin polymerization (Fig. 9 A). Under the conditions used, latrunculin B increased the secretory activity, while jasplakinolide had no significant effect on secretion. In latrunculin B–treated cells, the inhibitory effect of Rab27A-Q78L was significantly reduced compared with the one observed in the absence of drug (Fig. 9 B). Latrunculin B also reduced the effect of MyRIP. On the other hand, the inhibition of secretion induced by MyRIP overexpression was much stronger after jasplakinolide treatment than in standard conditions (Fig. 9 B). This effect is probably mediated by direct interaction of MyRIP with F-actin because it was not observed with MyRIP-ΔCter. The effect of granuphilin, another putative effector of Rab27A, was not increased by jasplakinolide (Fig. 9 B). In contrast to drugs that act on the actin cortex, microtubule depolymerization by nocodazole did not modify the effect of Rab27A and MyRIP (not depicted). The inhibitory effect of Rab27A and MyRIP, which does not by itself modify the actin cortex (not depicted), is thus partly dependent on the integrity and dynamics of the cytoskeleton.

Rab27A and MyRIP restrict granule motion
Evanescent wave fluorescence microscopy (EW-FM) allows observation of fluorescent markers in a thin optical section

near a glass–water interface. PC12 cells cultured on the glass interface were transfected with a NPY–GFP construct to label SGs and imaged with this technique. Under these conditions, the fluorescent SGs close to the plasma membrane were easily observed (Fig. 10 A), and their individual behavior was recorded with a CCD camera (Fig. 10 B). The intensity of the evanescent wave decreased exponentially with the distance from the interface with a decay constant in the cell adjusted to 200 nm. According to previous studies in PC12 cells (Lang et al., 2000), most of SGs imaged by this technique are located in the actin cortex.

The mobility of SGs in unstimulated cells was analyzed in 1-min sequences of 120 frames (Video 1, available at http://www.jcb.org/cgi/content/full/jcb.200302157/DC1). Most of the vesicles had limited movements (Fig. 10 B, arrowhead), but some moved on longer distances (Fig. 10 B, arrow). The x,y trajectories were monitored using a single particle tracking software (Fig. 10, C and D), and the mean x,y diffusion coefficients (Dx,y) were derived from mean square displacement (MSD) analysis.

Rab27A-Q78L or various MyRIP constructs were transiently expressed in PC12 cells together with NPY–GFP (see Videos 1–5 for representative examples, available at http://www.jcb.org/cgi/content/full/jcb.200302157/DC1). All SGs that could be followed for >15 s were tracked (150–700 SGs from 15–60 cells per group). Expression of
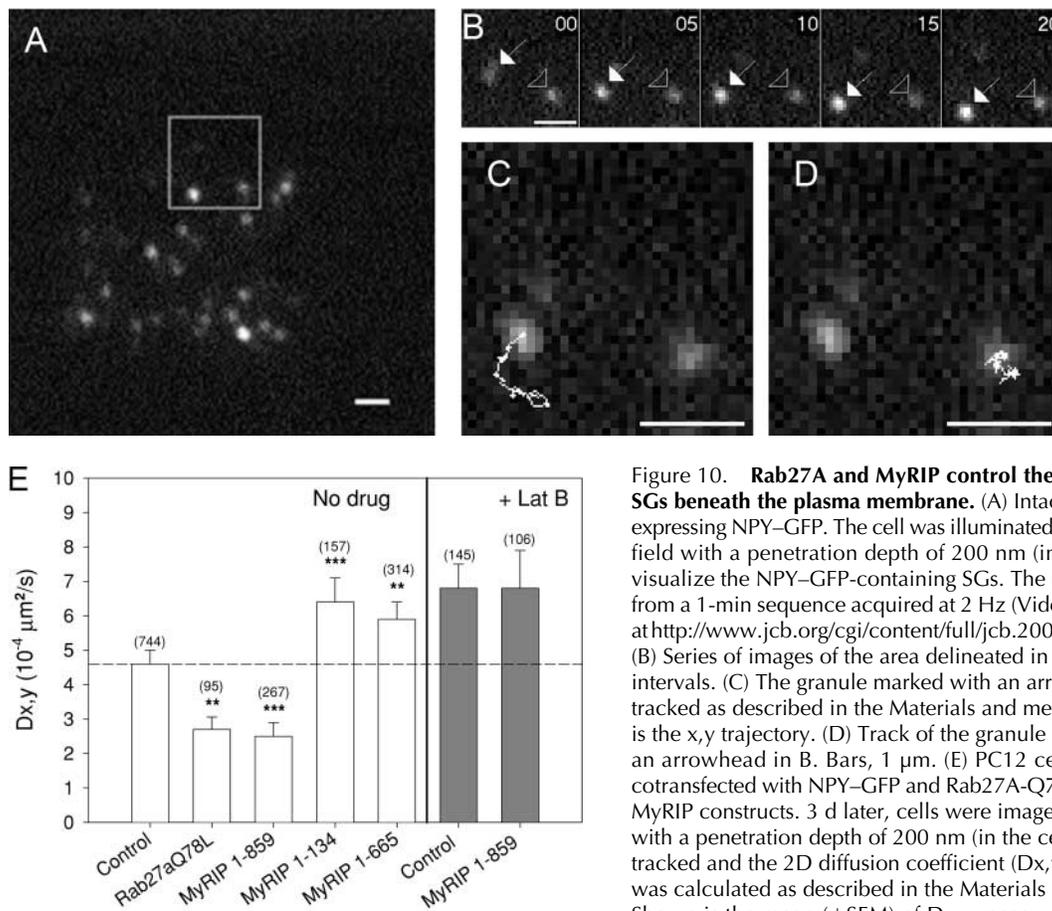
Figure 10. **Rab27A and MyRIP control the motion of SGs beneath the plasma membrane.** (A) Intact PC12 cell expressing NPY–GFP. The cell was illuminated by evanescent field with a penetration depth of 200 nm (in the cell) to visualize the NPY–GFP-containing SGs. The image is taken from a 1-min sequence acquired at 2 Hz (Video 5, available at http://www.jcb.org/cgi/content/full/jcb.200302157/DC1). (B) Series of images of the area delineated in A taken at 5-s intervals. (C) The granule marked with an arrow in B was tracked as described in the Materials and methods. Shown is the x,y trajectory. (D) Track of the granule marked with an arrowhead in B. Bars, 1 μm. (E) PC12 cells were cotransfected with NPY–GFP and Rab27A-Q78L or different MyRIP constructs. 3 d later, cells were imaged by EW-FM with a penetration depth of 200 nm (in the cell). SGs were tracked and the 2D diffusion coefficient (Dx,y) of each SG was calculated as described in the Materials and methods. Shown is the mean (±SEM) of Dx,y measured in mock-transfected (Control) and Rab27A-Q78L, MyRIP (1-859), MyRIP-RBD (1-134), and MyRIP-ΔCter (1-665) transfected cells. Latrunculin B (Lat B, right) increased the mean Dx,y of control cells. Moreover, under these conditions, the mobility of SGs from MyRIP-expressing cells was not different from that of mock-transfected cells. The number of tracked SGs is indicated above the bars. The significance of the differences was measured with Mann-Whitney U test.

Rab27A-Q78L or MyRIP clearly shifted the distribution of Dx,y toward lower values (not depicted) and lowered the mean diffusion coefficient (Fig. 10 E), indicating reduced mobility of SGs. In contrast, expression of MyRIP-RBD and MyRIP-ΔCter increased the mean diffusion coefficient. None of these proteins affected the mean number of SGs per area unit (unpublished data). In latrunculin-treated cells, SG mobility was enhanced but was insensitive to MyRIP overexpression (Fig. 10 E, right).

Discussion

The data presented here suggest that Rab27A and MyRIP provide a link between SGs and F-actin, and control short-range movements of SGs beneath the plasma membrane and their access to exocytotic sites. Our results indicate that MyRIP and Rab27A are associated with SGs. This conclusion is supported by different approaches. First, Rab27A cofractionates with VMAT2 and VAMP2 in sucrose gradients of chromaffin cell extracts. Second, Rab27A and MyRIP colocalize with chromogranins in confocal sections of PC12 and chromaffin cells. Third, Rab27A colocalizes with SGs by immunoelectron microscopy. Interestingly, in several cases, Rab27A-associated gold particles were found in

small clusters, suggesting that Rab27A may define microdomains on SGs, as was proposed for Rab5 on endosomes (Sönnichsen et al., 2000). The association of Rab27A with SGs is consistent with recent findings obtained by Fukuda et al. (2002a). Rab27A and Rab27B have also been found on insulin-containing granules (Yi et al., 2002; Zhao et al., 2002) or platelet-dense or α granules (Barral et al., 2002). Moreover, Rab27A is involved in the regulation of CTL exocytosis at the immunological synapse (Ménasché et al., 2000; Haddad et al., 2001; Stinchcombe et al., 2001). Therefore, Rab27A and maybe Rab27B are associated with a broad range of secretory vesicles, and not only with typical lysosome-related organelles.

In agreement with the localization of Rab27A on SGs, the Rab27A-binding protein MyRIP colocalized with Rab27A and SG markers. The granular localization of MyRIP depends on its NH_2-terminal Rab27A-binding domain because truncated constructs lacking this domain are mislocalized (El-Amraoui et al., 2002; Fig. 4 C).

Studies on Griscelli syndrome or *ashen* CTLs lacking Rab27A revealed a defect in lytic granule exocytosis, suggesting that Rab27A is an essential component of the secretory machinery. During completion of this study, Fukuda et al. (2002a) reported that overexpression of wild-type Rab27A

increased the secretory activity of PC12 cells. Similar effects of Rab27A on insulin secretion were also reported recently (Yi et al., 2002). In chromaffin and PC12 cells, we found by several approaches that Rab27A and, more especially, GTP-ase-deficient Rab27A (that is properly targeted to SGs; Fig. S2) reduced the magnitude of the secretory response (Figs. 5–9). Rab27A-Q78L reduced not only the amount of released secretory products but also the frequency of release events, as measured by carbon fiber amperometry. This apparent discrepancy might result from differences in assays used to measure secretion, from the relative importance of various Rab27A effectors in different cells, or from a rate-limiting effect of GTP hydrolysis by Rab27A. An increased probability of spontaneous fusion does not seem to account for the observed inhibition of stimulus-dependent release by Rab27A and Rab27A-Q78L, as was proposed recently by Schlüter et al. (2002) for Rab3A, another GTPase associated with SGs. Indeed, we did not detect any significant increase in release activity in the resting state.

Our observations suggest that MyRIP mediates, at least partly, the effect of Rab27A on secretion and provides a physical link between SGs and actin. Indeed, both proteins reduced the "sustained" component of release that involves recruitment of vesicles from the "reserve" pool. Moreover, both Rab27A- and MyRIP-induced effects on secretion were modulated by drugs that affect the actin cortex. Latrunculin B, which reduces the thickness of the actin cortex, also reduced the inhibitory effects of Rab27A-Q78L and MyRIP, while the actin-stabilizing drug jasplakinolide strongly strengthened the effect of MyRIP (Fig. 9). Finally, both MyRIP and Rab27A-Q78L restrict the motion of SGs in the actin-rich region of the cell imaged by EW-FM, whereas MyRIP-RBD and MyRIP-ΔCter, which are supposed to reduce the association of endogenous MyRIP with Rab27A, enhanced the mobility of SGs (Fig. 10 E). Latrunculin was found to increase SG mobility in mock-transfected cells, in agreement with F-actin acting as a barrier, and to prevent the effect of MyRIP on SG motion, in agreement with MyRIP tethering SGs to F-actin.

Previous studies revealed that SGs are captured at the cell periphery by a process involving both microfilaments and microtubules (Rudolf et al., 2001). MyRIP and Rab27A may play a role in SG capture similar to that of Rab27A/melanophilin/myosin-Va in the actin-dependent retention of melanosomes. However, if actin filaments may favor the retention of SGs at the cell periphery, they also hamper the diffusion of SGs toward the plasma membrane, as indicated by the increase in SG mobility and release induced by latrunculin. MyRIP may link SGs to actin via myosin-Va, which was recently shown to favor the dispersion of immature SGs within the actin cortex (Rudolf et al., 2003) and to be involved in secretion (Rosé et al. 2003). Recruitment of a molecular motor might indeed promote the motion of SGs within the actin cortex. MyRIP may also link SGs to actin filaments via a myosin-independent mechanism involving the COOH-terminal region of MyRIP (Fig. 4; Fig. S4, available at http://www.jcb.org/cgi/content/full/jcb.200302157/DC1). This region displays significant sequence similarity with the actin-binding domain of melanophilin, suggesting that MyRIP may also bind F-actin directly. Our data indicate that this myosin-independent binding of MyRIP to actin is responsible for the restricted mobility of SGs. Indeed, SG motion was reduced by MyRIP but increased by MyRIP-ΔCter, which binds to myosin-Va but not to actin (Fig. 4). The motion of SGs within the actin cortex thus depends on the dynamics of actin remodeling and of Rab27/MyRIP/actin interaction.

The inhibition of secretion observed upon expression of Rab27A or MyRIP is apparently correlated with the restricted motion of SGs within the actin cortex. In the case of MyRIP, both effects display the same dependence on actin organization. Clearly, increasing the degree of actin polymerization (by jasplakinolide) and the interaction of SGs with actin (by MyRIP) is detrimental to the secretory process, most likely by preventing the access of SGs to release sites. However, MyRIP-ΔCter, which increased SG mobility, also reduced the magnitude of the secretory response. In this case, the effect on secretion was not strengthened by jasplakinolide. This result suggests that MyRIP may interfere with the secretory process via another mechanism. This hypothesis deserves further study. It will also be interesting to investigate the putative function of MyRIP in other secreting cells such as CTLs and neurons.

Materials and methods

Materials

The rabbit anti-MyRIP antibody and the anti–myosin-VIIa antibody were described previously (El Amraoui et al., 2002). Anti-LYAAT and anti-VMAT2 rabbit antisera were provided by B. Gasnier and C. Sagné (CNRS, Institut de Biologie Physico-Chimique); the anti–chromogranin B monoclonal antibody was a gift of W. Huttner (Max Planck Institute of Molecular Cell Biology and Genetics, Dresden, Germany); the anti–myosin-Va was provided by R. Cheney (University of North Carolina, Chapel Hill, NC). Anti-Rab27A monoclonal antibody was from Transduction Laboratories; anti–chromogranin A/B polyclonal antibody was from Abcam; anti-VAMP2 was from Synaptic Systems; anti-actin was from Sigma-Aldrich; and the myc tag 9B11 antibody was from Cell Signaling Technology.

Plasmid encoding rat SERT (pcDNA3-SERT) and NPY–GFP were provided by R. Blakely (Vanderbilt University School of Medicine, Nashville, TN) and W. Almers (Oregon Health Sciences University, Portland, OR), respectively. pcDNA3-granuphilin was a gift of R. Regazzi (University of Lausanne, Lausanne, Switzerland). pEGFP-C1 was from BD Biosciences Clontech. Other plasmids encoding MyRIP and Rab27A constructs were described previously (El-Amraoui et al., 2002; Ménasché et al., 2003). Streptolysin-O and α-toxin were obtained from S. Bhakdi (Johannes Gutenberg University, Mainz, Germany) (Bhakdi et al., 1993). Latrunculin B and jasplakinolide were from Calbiochem. Other chemicals were purchased from Sigma-Aldrich.

Cell culture and transfection

Primary dissociated chromaffin cells from bovine adrenal medulla were prepared by retrograde collagenase perfusion and cultured as previously described (Darchen et al., 1990). PC12 cells were cultured and transfected as described previously (Schonn et al., 2003). Where indicated, NGF (50 μg/ml) was added to the culture medium. COS-7 cells were cultured in DME supplemented with 10% FBS at 37°C under 5% CO_2. Chromaffin and COS-7 cells were transfected by electroporation using Optimix electroporation kit (Equibio). In brief, freshly prepared cells were suspended in Optimix buffer A and collected by centrifugation (800 g, 10 min). Cells (1.5 × 10^6) were resuspended in 55 μl Optimix buffer B containing vector DNAs (5 μg). A single electric shock (PC12: 650 V/cm, 24 ms; COS: 625 V/cm, 8 × 3 ms) was applied using a PS10 electropulsator (Jouan). Electroporated cells were immediately recovered in warm culture medium and plated onto polylysine-coated glass coverslips. Experiments were generally performed 3 d after transfection.

Immunoelectron microscopy

PC12 and chromaffin cells were fixed with 2% paraformaldehyde in 0.2 M phosphate buffer, pH 7.4, for 1 h at room temperature. Cells were embedded in 10% gelatin, infused in 2.3 M sucrose, and frozen in liquid nitrogen

as described in detail previously (Raposo et al., 1997). Ultrathin cryosections were prepared with a Leica FCS ultracryomicrotome (Leica) and single and double immunogold labeled with a mouse monoclonal anti-Rab27A antibody and a rabbit polyclonal anti–chromogranin A/B according to Slot et al. (1991). A rabbit anti–mouse IgG was used after the first incubation with the monoclonal anti-Rab27A antibody. Protein A–gold conjugates (PAG 10 and PAG 15) were purchased from the Department of Cell Biology, Utrecht University, Utrecht, Netherlands. Relative quantitation of the immunogold labeling for Rab27A was performed directly under the electron microscope by counting 650 gold particles associated with the different subcellular compartments of PC12 cells. 560 granules were analyzed for the presence of Rab27A.

Interaction assays
GST and GST-MyRIP constructs were expressed in *E. coli* BL21 cells and purified by affinity chromatography onto glutathione–Sepharose (Amersham Biosciences) using standard procedures.

Pull Down. Myosin-VIIa tail (El Amraoui et al. 2002) was expressed in COS-7 cells. Transfected COS-7 cells or PC12 cells were scrapped, sonicated, and solubilized at 4°C for 30 min in a buffer containing 1% Triton X-100, 150 mM NaCl, 25 mM Tris-Cl, pH 7.5, 2 mM ATP, and a cocktail of proteases inhibitors. After centrifugation (12,000 g, 15 min), supernatants (0.5–1 mg protein) were incubated for 1 h at 4°C under agitation with 1 nmol of purified GST or GST–MyRIP constructs prebound to 150 μl glutathione–Sepharose beads. The beads were washed three times in 150 mM NaCl, 25 mM Tris-Cl, pH 7.5, and eluted in Laemmli sample buffer. Starting material and eluates were analyzed by SDS-PAGE and immunoblotting for the presence of myosin-Va or -VIIa.

Coimmunoprecipitation. COS-7 cells were transfected 2 d before the experiment with vectors encoding myc-tagged MyRIP or MyRIP-ΔCter (1–665). Cells were lysed as described above. Extracts were incubated with protein A–Sepharose beads (100 μl wet volume; Amersham Biosciences) conjugated with or without affinity-purified anti-MyRIP antibody. After three washes, the eluates were analyzed by SDS-PAGE and immunoblotting for the presence of MyRIP (with an anti–c-myc tag antibody) or actin.

Secretion assays
The [^{3}H]5-HT release assay has been described previously (Schonn et al., 2003). In brief, PC12 cells were transfected with the serotonin transporter SERT, loaded with [^{3}H]5-HT (5–20 Ci/mmol; Amersham Biosciences). Basal release was measured in Locke's solution containing (in mM) NaCl 154, KCl 5.5, glucose 5.6, NaHCO$_3$ 3.5, CaCl$_2$ 2.5, MgCl$_2$ 1.2, Hepes 15, and 0.2% BSA, pH 7.4, adjusted with NaOH supplemented with 1 μM clomipramine. Secretion was measured at 37°C in high K$^+$ Locke's solution (55 mM K$^+$ with Na$^+$ reduced to 104.5 mM) in the presence of 1 μM clomipramine. After 2–10 min, the radioactivity released in the medium and remaining in the cells was measured. Alternatively, cells were rinsed twice with Ca^{2+}-free Locke's solution and permeabilized for 4 min at 37°C with 20 μM digitonin or 22 U streptolysin-O in (in mM) potassium glutamate 139, Pipes 20, HEDTA 2, EGTA 2, free Mg^{2+} 1, ATP 2, plus 0.3% BSA and pH adjusted to 7 using KOH. Secretion was then elicited in the same medium supplemented with 30 μM free Ca^{2+}, for 5 min at 37°C. Free Ca^{2+} concentrations were calculated according to Föhr et al. (1993) using calcv.22 software. Where indicated, cells were treated with 1 μM jasplakinolide or 5 μM latrunculin B for 20 min before being stimulated to secrete (in the continuing presence of the drug). The hGH release assay and amperometric recordings were performed as described previously (Schonn et al., 2003).

EW-FM
An upright microscope (Olympus BX50WI) has been adapted to EW-FM by the prism approach (Axelrod, 1981). To excite fluorescence, light from an argon laser set at 488 nm (Spectra Physics 177-G02) entered radially a hemispheric BK7 glass prism and struck its planar face at a supercritical angle. The angle was adjustable by means of telecentric optics to be described elsewhere, and the evanescent field decay length was calculated assuming a refractive index of 1.37 for the cellular medium (experimentally determined). NPY–GFP-transfected PC12 cells cultured on polylysine-coated glass coverslips were observed in Locke's solution. Coverslips were optically coupled to the planar face of the prism with immersion oil (Carl Zeiss MicroImaging, Inc.). The laser intensity was attenuated to ∼1 mW, and illumination was restricted to image acquisition by a shutter coupled to the camera. The cells were observed through a water immersion objective 60X 0.9 NA (Olympus), and the images were captured with a CDD camera (Photometrics CoolSnap HQ; Roper Scientific). In the present work, frames were acquired at 2 Hz in stacks of 120 images. Exposure

times were of 100–300 ms, depending upon the signal to noise ratio, and under these conditions, <5% photobleaching occurred.

Analysis of SG motion
The positions of SGs in an x,y plane parallel to the membrane glass interface were determined using software modules provided by Metamorph (Universal Imaging). Occasionally, the image stacks were processed by a long pass filter (Steyer and Almers, 1999) before tracking the vesicles. For tracking, SGs that did not collide with neighboring granules and that stay bright for at least 30 images (15 s) were selected. A threshold brightness was then chosen, resulting in binary stacks where SGs appeared as single continuous regions of bright pixels. The position of the tracked SGs was determined as the mass center of these contiguous bright pixels. The trajectories were derived from the SG positions on each frame. For each SG trajectory, the MSD in the x,y plane was calculated according to Steyer and Almers (1999). Plots of MSD as a function of Δt were linear for Δt < 5 s, and a two-dimension diffusion constant Dx,y was derived from the slope of the curve.

Statistical analyses
Significance of differences was calculated with t test or Mann-Whitney U test; *, P < 0.05; **, P < 0.01; ***, P < 0.001.

Online supplemental material
The supplemental material (Figs. S1–S4, Videos 1–5, and supplemental Materials and methods) is available at http://www.jcb.org/cgi/content/full/jcb.200302157/DC1. Fig. S1 shows the presence of Rab27A in subcellular fractions enriched in SGs. Fig. S2 shows the distribution of Rab27A constructs in PC12 cells. Fig. S3 illustrates the cellular expression of the different constructs used in this study. Fig. S4 depicts how Rab27A and MyRIP may bridge SGs to actin. The videos illustrate the effect of Rab27A and MyRIP on SG motion. Plasmid constructions and protocols used for immunocytochemistry and subcellular fractionation are described in the supplemental Materials and methods.

References

Axelrod, D. 1981. Cell–substrate contacts illuminated by total internal reflection fluorescence. *J. Cell Biol.* 89:141–145.

Bahadoran, P., E. Aberdam, F. Mantoux, R. Busca, K. Bille, N. Yalman, G. de Saint-Basile, R. Casaroli-Marano, J.P. Ortonne, and R. Ballotti. 2001. Rab27a: a key to melanosome transport in human melanocytes. *J. Cell Biol.* 152:843–850.

Barral, D.C., J.S. Ramalho, R. Anders, A.N. Hume, H.J. Knapton, T. Tolmachova, L.M. Collinson, D. Goulding, K.S. Authi, and M.C. Seabra. 2002. Functional redundancy of Rab27 proteins and the pathogenesis of Griscelli syndrome. *J. Clin. Invest.* 110:247–257.

Bhakdi, S., U. Weller, I. Walev, E. Martin, D. Jonas, and M. Palmer. 1993. A guide to the use of pore-forming toxins for controlled permeabilization of cell membranes. *Med. Microbiol. Immunol. (Berl.).* 182:167–175.

Darchen, F., A. Zahraoui, F. Hammel, M.P. Monteils, A. Tavitian, and D. Scherman. 1990. Association of the GTP-binding protein Rab3A with bovine adrenal chromaffin granules. *Proc. Natl. Acad. Sci. USA.* 87:5692–5696.

Denzer, K., M.J. Kleijmeer, H.F. Heijnen, W. Stoorvogel, and H.J. Geuze. 2000. Exosome: from internal vesicle of the multivesicular body to intercellular signaling device. *J. Cell Sci.* 113(Pt 19):3365–3374.

El-Amraoui, A., J.S. Schonn, P. Kussel-Andermann, S. Blanchard, C. Desnos, J.P. Henry, U. Wolfrum, F. Darchen, and C. Petit. 2002. MyRIP, a novel Rab effector, enables myosin VIIa recruitment to retinal melanosomes. *EMBO Rep.* 3:463–470.

Föhr, K.J., W. Warchol, and M. Gratzl. 1993. Calculation and control of free divalent cations in solutions used for membrane fusion studies. *Methods Enzymol.* 221:149–157.

Fukuda, M., and T.S. Kuroda. 2002. Slac2-c (synaptotagmin-like protein homo-

logue lacking C2 domains-c), a novel linker protein that interacts with Rab27, myosin Va/VIIa, and actin. *J. Biol. Chem.* 277:43096–43103.

Fukuda, M., E. Kanno, C. Saegusa, Y. Ogata, and T.S. Kuroda. 2002a. Slp4-a/granuphilin-a regulates dense-core vesicle exocytosis in PC12 cells. *J. Biol. Chem.* 277:39673–39678.

Fukuda, M., T.S. Kuroda, and K. Mikoshiba. 2002b. Slac2-a/melanophilin, the missing link between Rab27 and myosin Va: implications of a tripartite protein complex for melanosome transport. *J. Biol. Chem.* 277:12432–12436.

Haddad, E.K., X. Wu, J.A. Hammer III, and P.A. Henkart. 2001. Defective granule exocytosis in Rab27a-deficient lymphocytes from Ashen mice. *J. Cell Biol.* 152:835–842.

Hume, A.N., L.M. Collinson, A. Rapak, A.Q. Gomes, C.R. Hopkins, and M.C. Seabra. 2001. Rab27a regulates the peripheral distribution of melanosomes in melanocytes. *J. Cell Biol.* 152:795–808.

Hume, A.N., L.M. Collinson, C.R. Hopkins, M. Strom, D.C. Barral, G. Bossi, G.M. Griffiths, and M.C. Seabra. 2002. The leaden gene product is required with Rab27a to recruit myosin Va to melanosomes in melanocytes. *Traffic.* 3:193–202.

Johannes, L., P.M. Lledo, M. Roa, J.D. Vincent, J.P. Henry, and F. Darchen. 1994. The GTPase Rab3a negatively controls calcium-dependent exocytosis in neuroendocrine cells. *EMBO J.* 13:2029–2037.

Lang, T., I. Wacker, I. Wunderlich, A. Rohrbach, G. Giese, T. Soldati, and W. Almers. 2000. Role of actin cortex in the subplasmalemmal transport of secretory granules in PC-12 cells. *Biophys. J.* 78:2863–2877.

Matesic, L.E., R. Yip, A.E. Reuss, D.A. Swing, T.N. O'Sullivan, C.F. Fletcher, N.G. Copeland, and N.A. Jenkins. 2001. Mutations in Mlph, encoding a member of the Rab effector family, cause the melanosome transport defects observed in leaden mice. *Proc. Natl. Acad. Sci. USA.* 98:10238–10243.

Ménasché, G., E. Pastural, J. Feldmann, S. Certain, F. Ersoy, S. Dupuis, N. Wulffraat, D. Bianchi, A. Fischer, F. Le Deist, and G. de Saint Basile. 2000. Mutations in RAB27A cause Griscelli syndrome associated with haemophagocytic syndrome. *Nat. Genet.* 25:173–176.

Ménasché, G., J. Feldmann, A. Houdusse, C. Desaymard, A. Fischer, B. Goud, and G. de Saint Basile. 2003. Biochemical and functional charaterization of Rab27a mutations occurring in Griscelli syndrome patients. *Blood.* 101:2736–2742.

Nakata, T., and N. Hirokawa. 1992. Organization of cortical cytoskeleton of cultured chromaffin cells and involvement in secretion as revealed by quickfreeze, deep-etching, and double-label immunoelectron microscopy. *J. Neurosci.* 12:2186–2197.

Oheim, M., and W. Stuhmer. 2000. Tracking chromaffin granules on their way through the actin cortex. *Eur. Biophys. J.* 29:67–89.

Ornberg, R.L., L.T. Duong, and H.B. Pollard. 1986. Intragranular vesicles: new organelles in the secretory granules of adrenal chromaffin cells. *Cell Tissue Res.* 245:547–553.

Provance, D.W., Jr., M. Wei, V. Ipe, and J.A. Mercer. 1996. Cultured melanocytes from dilute mutant mice exhibit dendritic morphology and altered melanosome distribution. *Proc. Natl. Acad. Sci. USA.* 93:14554–14558.

Raposo, G., M.J. Kleijmeer, G. Posthuma, J.W. Slot, and H.J. Geuze. 1997. Immunogold labeling of ultrathin cryosections: application in immunology. *In* Handbook of Experimental Immunology. 5th ed. Vol. 4. L.A. Herzenberg, D. Weir, C. Blackwell, editors. Blackwell Science, Cambridge, MA. 1–11.

Rosé, S.D., T. Lejen, L. Casaletti, R.E. Larson, T.D. Pene, and J.M. Trifaro. 2003. Myosins II and V in chromaffin cells: myosin V is a chromaffin vesicle molecular motor involved in secretion. *J. Neurochem.* 85:287–298.

Rudolf, R., T. Salm, A. Rustom, and H.H. Gerdes. 2001. Dynamics of immature secretory granules: role of cytoskeletal elements during transport, cortical restriction, and F-actin-dependent tethering. *Mol. Biol. Cell.* 12:1353–1365.

Rudolf, R., T. Kogel, S.A. Kuznetsov, T. Salm, O. Schlicker, A. Hellwig, J.A. Hammer III, and H.H. Gerdes. 2003. Myosin Va facilitates the distribution of secretory granules in the F-actin rich cortex of PC12 cells. *J. Cell Sci.* 116:1339–1348.

Sagné, C., C. Agulhon, P. Ravassard, M. Darmon, M. Hamon, S. El Mestikawy, B.

Gasnier, and B. Giros. 2001. Identification and characterization of a lysosomal transporter for small neutral amino acids. *Proc. Natl. Acad. Sci. USA.* 98:7206–7211.

Schlüter, O.M., M. Khvotchev, R. Jahn, and T.C. Sudhof . 2002. Localization versus function of Rab3 proteins. Evidence for a common regulatory role in controlling fusion. *J. Biol. Chem.* 277:40919–40929.

Schonn, J.S., C. Desnos, J.P. Henry, and F. Darchen. 2003. Transmitter uptake and release in PC12 cells overexpressing plasma membrane monoamine transporters. *J. Neurochem.* 84:669–677.

Slot, J.W., H.J. Geuze, S. Gigengack, G.E. Lienhard, and D. James. 1991. Immuno-localization of the insulin regulatable glucose transporter in brown adipose tissue of the rat. *J. Cell Biol.* 113:123–135.

Sönnichsen, B., S. De Renzis, E. Nielsen, J. Rietdorf, and M. Zerial. 2000. Distinct membrane domains on endosomes in the recycling pathway visualized by multicolor imaging of Rab4, Rab5, and Rab11. *J. Cell Biol.* 149:901–914.

Spector, I., N.R. Shochet, Y. Kashman, and A. Groweiss. 1983. Latrunculins: novel marine toxins that disrupt microfilament organization in cultured cells. *Science.* 219:493–495.

Steyer, J.A., and W. Almers. 1999. Tracking single secretory granules in live chromaffin cells by evanescent-field fluorescence microscopy. *Biophys. J.* 76:2262–2271.

Stinchcombe, J.C., D.C. Barral, E.H. Mules, S. Booth, A.N. Hume, L.M. Machesky, M.C. Seabra, and G.M. Griffiths. 2001. Rab27a is required for regulated secretion in cytotoxic T lymphocytes. *J. Cell Biol.* 152:825–834.

Strobel, M.C., P.K. Seperack, N.G. Copeland, and N.A. Jenkins. 1990. Molecular analysis of two mouse dilute locus deletion mutations: spontaneous dilute lethal20J and radiation-induced dilute prenatal lethal Aa2 alleles. *Mol. Cell. Biol.* 10:501–509.

Strom, M., A.N. Hume, A.K. Tarafder, E. Barkagianni, and M.C. Seabra. 2002. A family of Rab27-binding proteins: melanophilin links Rab27a and myosin Va function in melanosome transport. *J. Biol. Chem.* 277:25423–25430.

Trifaro, J., S.D. Rose, T. Lejen, and A. Elzagallaai. 2000. Two pathways control chromaffin cell cortical F-actin dynamics during exocytosis. *Biochimie.* 82:339–352.

Wick, P.F., R.A. Senter, L.A. Parsels, M.D. Uhler, and R.W. Holz. 1993. Transient transfection studies of secretion in bovine chromaffin cells and PC12 cells. Generation of kainate-sensitive chromaffin cells. *J. Biol. Chem.* 268:10983–10989.

Wightman, R.M., J.A. Jankowski, R.T. Kennedy, K.T. Kawagoe, T.J. Schroeder, D.J. Leszczyszyn, J.A. Near, E.J. Diliberto, Jr., and O.H. Viveros. 1991. Temporally resolved catecholamine spikes correspond to single vesicle release from individual chromaffin cells. *Proc. Natl. Acad. Sci. USA.* 88:10754–10758.

Wilson, S.M., R. Yip, D.A. Swing, T.N. O'Sullivan, Y. Zhang, E.K. Novak, R.T. Swank, L.B. Russell, N.G. Copeland, and N.A. Jenkins. 2000. A mutation in Rab27a causes the vesicle transport defects observed in ashen mice. *Proc. Natl. Acad. Sci. USA.* 97:7933–7938.

Wu, X., B. Kocher, Q. Wei, and J.A. Hammer III. 1998. Myosin Va associates with microtubule-rich domains in both interphase and dividing cells. *Cell Motil. Cytoskeleton.* 40:286–303.

Wu, X., K. Rao, M.B. Bowers, N.G. Copeland, N.A. Jenkins, and J.A. Hammer III. 2001. Rab27a enables myosin Va-dependent melanosome capture by recruiting the myosin to the organelle. *J. Cell Sci.* 114:1091–1100.

Wu, X.S., K. Rao, H. Zhang, F. Wang, J.R. Sellers, L.E. Matesic, N.G. Copeland, N.A. Jenkins, and J.A. Hammer III. 2002. Identification of an organelle receptor for myosin-Va. *Nat. Cell Biol.* 4:271–278.

Yi, Z., H. Yokota, S. Torii, T. Aoki, M. Hosaka, S. Zhao, K. Takata, T. Takeuchi, and T. Izumi. 2002. The Rab27a/granuphilin complex regulates the exocytosis of insulin-containing dense-core granules. *Mol. Cell. Biol.* 22:1858–1867.

Zhao, S., S. Torii, H. Yokota-Hashimoto, T. Takeuchi, and T. Izumi. 2002. Involvement of Rab27b in the regulated secretion of pituitary hormones. *Endocrinology.* 143:1817–1824.